# Ferromagnetic semiconductors

## Tomasz Dietl

Institute of Physics, Polish Academy of Sciences, al. Lotników 32/46,
PL-02-668 Warszawa, Poland

E-mail: dietl@ifpan.edu.pl

## Abstract
The current status and prospects of research on ferromagnetism in semiconductors are reviewed. The question of the origin of ferromagnetism in europium chalcogenides, chromium spinels and, particularly, in diluted magnetic semiconductors is addressed. The nature of electronic states derived from 3d of magnetic impurities is discussed in some detail. Results of a quantitative comparison between experimental and theoretical results, notably for Mn-based III–V and II–VI compounds, are presented. This comparison demonstrates that the current theory of the exchange interactions mediated by holes in the valence band describes correctly the values of Curie temperatures $T_C$, magnetic anisotropy, domain structure and magnetic circular dichroism. Furthermore, chemical trends are discussed and lead to the prediction of semiconductor systems with $T_C$ that may exceed room temperature. This expectation is being confirmed by recent findings. Results for materials containing magnetic ions other than Mn are also presented emphasizing that the double exchange involving hopping through d states may operate in those systems.

## 1. Introduction

Because of the complementary properties of semiconductor and ferromagnetic material systems, a growing effort is directed toward studies of semiconductor-magnetic nanostructures. Applications in optical modulators and insulators, in sensors and memories [1], as well as for computing using electron spins [2] can be envisaged. The hybrid nanostructures, in which both electric and magnetic field are spatially modulated, are usually fabricated by patterning of a ferromagnetic metal on the top of a semiconductor [3] or by inserting ferromagnetic dots or layers into a semiconductor matrix [4]. In such devices, the stray fields can control charge and spin dynamics in the semiconductor. At the same time, spin-polarized electrons in the metal can be injected into or across the semiconductor [5]. Furthermore, the ferromagnetic neighbours may affect semiconductor electronic states by the ferromagnetic proximity effect even under thermal equilibrium conditions. Particularly perspective materials in the context of hybrid structures appear to be those elemental or compound ferromagnets which can be grown in the same reactor as the semiconductor counterpart.

The early studies of Cr spinels [6], rock-salt Eu- [7–11] and Mn-based [12] chalcogenides led to the observation of a number of outstanding phenomena associated with the interplay between ferromagnetic cooperative phenomena and semiconducting properties. The discovery of ferromagnetism in zinc-blende III–V [13, 14] and II–VI [15, 16] Mn-based compounds allows one to explore the physics of previously unavailable combinations of quantum structures and magnetism in semiconductors. For instance, the possibility of changing the magnetic phase isothermally, by light [15, 17, 18] or by electric field [19, 20], was put into the evidence in (In,Mn)As/(Al,Ga)Sb [17, 19] and (Cd,Mn)Te/(Cd,Zn,Mg)Te [15, 18, 20] heterostructures. The injection of spin-polarized carriers from (Ga,Mn)As to a (In,Ga)As quantum well in the absence of an external magnetic field was demonstrated too [21]. At the same time, outstanding phenomena, known from the earlier studies of metallic multilayer structures, have also been observed in ferromagnetic semiconductors, examples being interlayer coupling [22, 23], exchange bias-type behaviour [24], giant [22] and tunnelling magnetoresistance [25]. It is then the important challenge of materials science to understand the ferromagnetism in these compounds and to develop functional semiconductor systems with the Curie temperatures $T_C$ exceeding comfortably the room temperature.

We begin this review by describing briefly, in section 2, various families of ferromagnetic semiconductors and theoretical models proposed to explain the nature of relevant spin–spin exchange interactions. We then discuss, in section 3,

energies and characteristics of electronic states derived from 3d shells of magnetic impurities in II–VI and III–V semiconductors, which provide information on the charge and spin states as well as on the effect of the magnetic constituent on the carrier concentration, also in the presence of co-doping by shallow donors or acceptors. In section 4, we outline the main ingredients and limitations of the mean-field Zener model recently put forward to describe quantitatively the hole-mediated ferromagnetism in tetrahedrally coordinated semiconductors [26–28]. Results of a quantitative comparison between experimental and theoretical results for Mn-based III–V and II–VI compounds are shown in section 5. This comparison demonstrates that the current theory of the exchange interactions mediated by holes in the valence band describes correctly the values of $T_C$, magnetic anisotropy, and domain structure. Finally, in section 6, we present the theoretically predicted chemical trends and discuss various suggestions concerning the design of high-temperature ferromagnetic semiconductors.

The novel physics of magnetic heterostructures constitutes the topic of the next paper [29] in this special issue and, therefore, is not discussed here. There are, of course, a number of other recent review articles describing many aspects of ferromagnetic III–V [30–32], II–VI [33, 34], and IV–VI materials [12], which are not touched upon in this paper.

## 2. Families of ferromagnetic semiconductors and relevant spin–spin exchange interactions

Manganites (perovskite: (La,Sr)MnO$_3$ and related materials), which show colossal magnetoresistance, are magnetic semiconductors, whose studies have been particularly active over recent years [35, 36]. Their ferromagnetic order, beginning at 350 K, is brought by the double-exchange interaction involving on-site Hund's ferromagnetic spin coupling and hopping of d electrons between Mn$^{3+}$ and Mn$^{4+}$ ions.

The family of magnetic semiconductors also encompasses europium and chromium chalcogenides (rock-salt type: EuS, EuO and spinels: CdCr$_2$S$_4$, CdCr$_2$Se$_4$), for which the Curie temperature $T_C$ does not exceed 100 K. In the case of rock-salt Eu compounds, there appears to be competition between antiferromagnetic cation–anion–cation and ferromagnetic cation–cation superexchange [9]. The latter can be traced back to the ferromagnetic s–f coupling, and the presence of s–f hybridization, which is actually stronger than the p–f hybridization due to symmetry reasons [9, 37]. In such a situation, the lowering of the conduction band associated with the ferromagnetic order enhances the energy gain due to hybridization. The Cr-spinels represent the case, in which the d orbitals of the two cations are not coupled to the same p orbital, which results in a ferromagnetic superexchange.

In europium and chromium chalcogenides discussed above, the presence of carriers can affect $T_C$ but is not necessary for the appearance of the ferromagnetic order. In contrast, in the case of Mn-based IV–VI [12], III–V [38], and II–VI [39] diluted magnetic semiconductors (DMS) the ferromagnetism can be observed provided that the hole concentration is sufficiently high. According to experimental

and theoretical results, which are summarized in the next section, the ferromagnetic order in Mn-based DMS is mediated by carriers residing in relatively wide valence bands. In the case of III–V and II–VI DMS, the holes are coupled to the localized spins via a strong, symmetry allowed, antiferromagnetic p–d interaction. This is in contrast to manganites, where only d electrons in narrow bands appear to be involved. However, the d levels of transition metals other than Mn reside in the band gap of III–V and II–VI compounds. In such a situation the double exchange may constitute the dominant mechanism of spin–spin interactions.

## 3. Magnetic impurities in II–VI and III–V compounds

### 3.1. Energy levels

We consider tetrahedrally coordinated semiconductors, in which the magnetic ion occupies the cation sublattice, as found by extended x-ray absorption fine structure (EXAFS) studies in the case of Cd$_{1-x}$Mn$_x$Te [40] and Ga$_{1-x}$Mn$_x$As [41]. Obviously, magnetic properties of a semiconductor containing magnetic ion will depend on energetic positions of states derived from magnetic shells as well as on their interactions with the host bands. Furthermore, the energy of the magnetic levels in respect to host bands together with the on-site correlation energy $U$ determine whether the magnetic ion acts as a dopant and how its charge and spin state depends on the presence of other impurities.

According to the internal reference rule [42], the positions of states derived from magnetic shells do not vary across the entire family of the II–VI or III–V compounds if the valence band offsets between different compounds are taken into account. In figure 1, adapted from [43], the data for II–VI and III–V DMS containing various transition metals are collected. The symbols D(0/+) and A(0/−) denote the donor and acceptor levels derived from 3d shells of magnetic ions. In the case of II–VI DMS (left panel), these states correspond to the transformation of the doubly ionized magnetic ions M$^{2+}$ into M$^{3+}$ and into M$^{1+}$ ions, in their ground states, respectively, that is to the lower and upper Hubbard bands. Similarly, in the case of III–V DMS (right panel) D(0/+) and A(0/−) denote the donor and acceptor states which, however, in contrast to the situation in II–VI DMS, correspond to the transformation of the triply ionized magnetic ions M$^{3+}$ into M$^{4+}$ and into M$^{2+}$ ions, respectively. A characteristic evolution of the level energies with the number of the d electrons is seen in both II–VI and III–V DMS, the pattern known from atomic spectra but significantly flattened out in solids by screening and hybridization effects [44].

It should be noted at this point that the internal reference rule may serve only for the illustration of chemical trends and not for extracting the precise values of the ionization energies. Moreover, the interaction between the impurity and host states can lead to the appearance of additional band-gap levels derived from the semiconductor bands. This may cause some ambiguity concerning the nature of localized states observed experimentally in these systems. In particular, a strong p–d hybridization can lead to a binding of a hole in
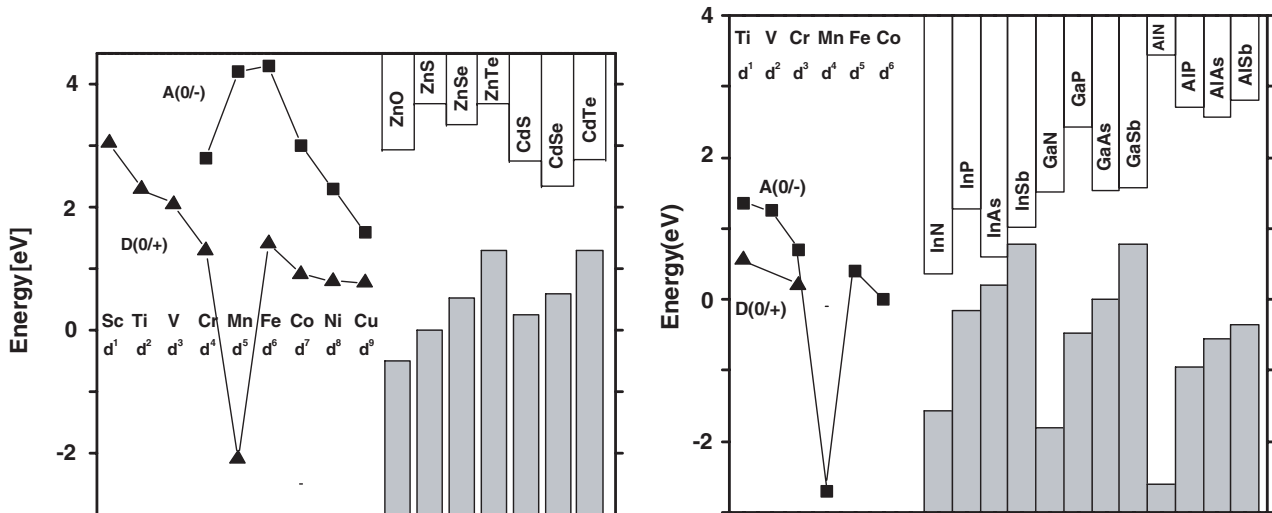
**Figure 1.** Approximate positions of transition metals levels relative to the conduction and valence band edges of II–VI (left panel) and III–V (right panel) compounds. By triangles the $d^N/d^{N-1}$ donor and by squares the $d^N/d^{N+1}$ acceptor states are denoted (adapted from [43]).

a Zhang–Rice polaron (charge transfer) state, which then gives rise to an additional level in the band gap [45–49]. Furthermore, if the $d^N/d^{N-1}$ donor state resides above the bottom of the conduction band, the ground state corresponds to a hydrogenic-like level $d^{N-1}+e$ located below the band edge, as observed in CdSe:Sc [50]. Similarly, if the acceptor state lies under the top of the valence band, the ground state corresponds to a hydrogenic-like acceptor $d^{N+1}+h$, not to the $d^N$ state. Importantly, band carriers introduced by such magnetic ions can mediate exchange interactions between the parent spins. Obviously, energies of hydrogenic-like states follow the band edges, and by no means are described by the internal reference rule. This appears to be the situation of the Mn related levels in the gap of III–V compounds [49], the case discussed in detail below.

### 3.2. Mn in II–VI compounds

It is well established that Mn is divalent in II–VI compounds, and assumes the high spin $d^5$ configuration characterized by $S = 5/2$ and $g = 2.0$ [51–53]. Indeed, according to figure 1, the Mn ions neither introduce nor bind carriers, but give rise to the presence of the localized spin in II–VI DMS. The spin dependent hybridization between anion p and Mn d states leads to the superexchange, a short-range antiferromagnetic coupling among the Mn moments. In order to take the influence of this interaction into account, it is convenient to parametrize the dependence of magnetization on the magnetic field in the absence of the carriers, $M_o(H)$, by the Brillouin function, in which two empirical parameters, the effective spin concentration $x_{eff}N_0 < xN_0$ and temperature $T_{eff} > T$, take the presence of the superexchange interactions into account [52, 53]. The dependencies $x_{eff}(x)$ and $T_{AF}(x) \equiv T_{eff}(x) - T$ have been determined for a number of Mn-based II–VI DMS. Importantly, the antiferromagnetic superexchange can be overcompensated by ferromagnetic interactions mediated by band holes [26], the theoretical prediction confirmed subsequently by the observation of ferromagnetic ordering in p-type II–VI DMS [15, 16].
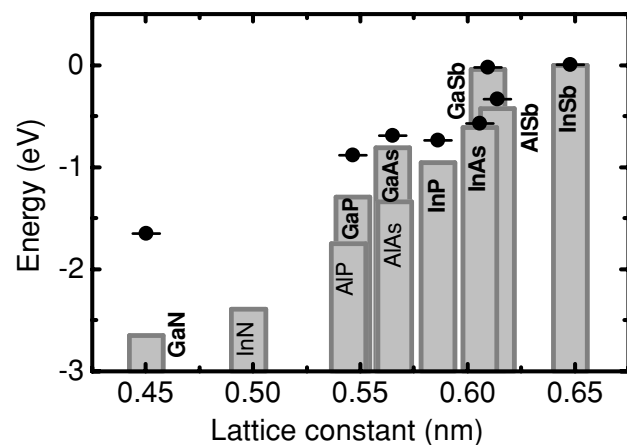


**Figure 2.** Experimental energies of Mn levels in the gap of III–V compounds according to in respect to valence-band edges, whose relative positions are taken from [151] (after [49]).

### 3.3. Mn in III–V compounds

Figure 2, taken from [49], shows the energetic position of the Mn impurity level in III–V compounds, as evaluated by various authors from measurements of optical spectra and activation energy of conductivity. *A priori*, the Mn atom, when substituting a trivalent metal, may assume either of two configurations: (i) $d^4$ or (ii) $d^5$ plus a weakly bound hole, $d^5+h$. Accordingly, the experimentally determined energies correspond to either $d^4/d^5$ or $d^5+h/d^5$ levels.

It appears to be a general consensus that the Mn acts as an effective mass acceptor ($d^5+h$) in the case of antimonides and arsenides. Such a view is supported by the relatively small Mn concentrations leading to the insulator-to-metal transition, which according to the Mott criterion $n^{1/3}a_B = 0.26$, points to a relatively large extension of the effective Bohr radius $a_B$. Moreover, the ESR studies of GaAs:Mn reveal, in addition to the well known spectrum of Mn $d^5$ with the Landé factor

379

$g_{Mn} = 2.0$, two additional lines corresponding to $g_1 = 2.8$ and $g_2 \approx 6$ [54–56], which can be described quantitatively within the $k \cdot p$ scheme for the occupied acceptor [54, 55]. Here, the presence of a strong antiferromagnetic p–d exchange interaction between the bound hole and the Mn d-electrons has to be assumed, so that the total momentum of the complex is $J = 1$. In agreement with the model, the additional ESR lines, in contrast to the $g = 2.0$ resonance, are visible only in a narrow range of the Mn concentration [56]. This range should be greater than the concentration of compensating donors, and smaller than that at which acceptor wavefunctions start to overlap and merge with the valence band. The antiferromagnetic coupling within the $d^5+h$ complex is seen in a number of experiments, and has been employed to evaluate the p–d exchange integral $\beta N_0 \approx -1\,eV$ [57] in GaAs:Mn, the value in agreement with that determined from interband magnetoabsorption in (Ga,Mn)As [58].

Importantly, the above scenario is corroborated by results of photoemission [59, 60] and x-ray magnetic circular dichroism (XMCD) studies [61, 62] in metallic or nearly metallic (Ga,Mn)As. The latter point to the $d^5$ Mn configuration. The former are not only consistent with such a configuration but also lead to the value of $\beta N_0$ similar to that quoted above, $\beta N_0 \approx -1.2\,eV$ [59]. Furthermore, the photoemission reveals the presence of two features in the density of states brought about by the Mn constituent: the original Mn $3d^5$ states located around 4.5 eV below the Fermi energy $E_F$, and new states merging with the valence band in the vicinity of $E_F$ [60]. These new states correspond to acceptors, as discussed above. They are derived from the valence band by the Coulomb field as well as by a local Mn potential that leads to a chemical shift in the standard impurity language, or to a valence band offset in the alloy nomenclature.

In contrast to antimonides and arsenides, the situation is much more intricate in the case of phosphides and nitrides. Here, ESR measurements reveal the presence of a line with $g = 2.0$ only [63–66], which is thus assigned to $d^5$ centres [64–66]. Moreover, according to a detailed study carried out for a compensated n-type GaP:Mn [65], the ESR amplitude diminishes under illumination and, simultaneously, new lines appear, a part of which exhibit anisotropy consistent with the $d^4$ configuration. This, together with the apparent lack of evidence for $d^5+h$ states, even in p-type materials, seems to imply that Mn in the ground state possesses the $d^4$, not $d^5+h$, electron configuration [65]. This would mean that the Mn energy in figure 2 for GaP [65] and, therefore, for GaN [67, 68] (where the valence band is lower than in GaP) corresponds to the $d^4/d^5$, not $d^5+h/d^5$ level. Such a view appears to be supported by the *ab initio* computation within the local spin density approximation (LSDA), which points to the presence of the d-states in the gap of (Ga,Mn)N [69]. In this situation, the spin–spin interaction would be driven by a double exchange mechanism involving hopping of d-electrons [69, 70], as in the case of colossal magnetoresistance manganites, not by the holes in the valence band.

However, the above interpretation has recently been called into question [49]. In particular, guided by photoemission results for II–VI compounds [48] one expects that the energy of the $d^4/d^5$ level will vary little between arsenides and nitrides. This implies that this level should reside in the valence band

of GaN despite the 1.8 eV valence band offset between GaN and GaAs, as shown in figure 1. The resulting contradiction with the LSDA findings can be removed by noting that in the case of strongly correlated 3d electrons, a semi-empirical LSDA+U approach is necessary to reconcile the computed and photoemission positions of states derived from the Mn 3d shell in (Ga,Mn)As [60, 71].

Another important aspect of magnetic acceptors is that the p–d hybridization, in addition to producing the exchange interaction, can contribute to the hole binding energy $E_b$. By taking the hole wavefunction as a coherent superposition of p-states of anions adjacent to Mn [45] and assuming the p-orbitals to be directed towards the Mn ion, the $T_2$ state has been found to have 30% lower energy than that corresponding to the mutually parallel p-orbitals [49]. This shows that the Kohn–Luttinger amplitudes away from the $\Gamma$ point of the Brillouin zone are also involved. In order to evaluated $E_b$, a square-well spherical potential $V(r) = V_o\Theta(b-r)$ is assumed [47], whose depth $V_o$ is determined by the p–d hybridization taking into account the above mentioned arrangement of the p-orbitals,

$$V_o = \frac{5}{8\pi}\frac{\beta N_0}{1.04}\left(1 - \frac{\Delta_{\text{eff}}}{U_{\text{eff}}}\right)\left(\frac{a_o}{b}\right)^3. \quad (1)$$

Here, the values of $\beta N_0$ are taken from [28]; $\Delta_{\text{eff}}$ is the distance of $d^4/d^5$ level to the top of the valence band, which is evaluated to be 2.7 eV in (Ga,Mn)As [59], and is assumed to be reduced in other compounds by the corresponding valence band offsets, and $U_{\text{eff}} = 7\,eV$ is the correlation energy of the 3d electrons [48, 59], the energies visible in figures 1 and 2. Finally, $b/a_o$ is the well radius in the units of the lattice constant, and should lie in-between the cation–anion and cation–cation distance, $\sqrt{3}a_o/4 < b < a_o/\sqrt{2}$. It turns out that in the case of GaN:Mn the hole is bound by Mn, even in the absence of the Coulomb potential, $E_b = 1.0$ eV for $b = 0.46a_o$. This demonstrates rather convincingly that a large part of $E_b$ originates indeed from the p–d interaction, indicating that the Zhang–Rice (ZR) limit [45, 47] is reached in these systems. One of the important consequences of the ZR polaron formation is the shift of the Mott critical concentration towards rather high values. According to the known relation between $E_b$ and $a_B$ [72], the critical hole concentration is $p_c = 4\times10^{19}$ cm$^{-3}$ in (Ga,Mn)As and at least an order of magnitude greater in (Ga,Mn)N, if no shallower acceptors are present.

## 4. Theoretical description of Mn-based ferromagnetic semiconductors

### 4.1. Electronic states and models of carrier-mediated ferromagnetism

Despite the considerable effort aimed at elucidating the nature of ferromagnetism in Mn-based II–VI and III–V DMS, the form of the relevant minimal Hamiltonian and its universality for all compounds are still under an active debate. Such a situation reflects the multifaceted environment, in which the ferromagnetism appears. Indeed, conceptual and technical difficulties inherent to theory of strongly correlated and disordered transition-metal compounds are combined—in

ferromagnetic semiconductors—with the intricate physics of Anderson–Mott localization and disordered Stoner magnetism that are specific to heavily doped semiconductors. Moreover, low-temperature epitaxy, by which III–V materials are obtained, results in a large concentration of native defects such as antisites, which act as compensating donors. Another possible source of local bonds reconstructions is the mechanism of self-compensation, occurring in heavily doped semiconductors once the Fermi level reaches the energy triggering defect reactions. Structural faults may form with neighbour transition metal impurities defect complexes exhibiting hitherto non-explored magnetic characteristics. At the same time, strong compensation by donor-like defects enhances the electrostatic disorder substantially, leading to deep and long-range potential fluctuations that result in significant band tailing.

There are two basic approaches to theoretical modelling of the materials in question: (i) *ab initio* or first principles studies and (ii) theories starting from effective Hamiltonians containing experimentally determined parameters. Since *ab initio* works are reviewed elsewhere [73], they will not be discussed here except for noting that they raise interesting questions to what extend the local spin density approximation (LSDA) can handle strong correlation inherent to charge-transfer and Hubbard–Mott insulators as well as whether the coherent potential approximation (CPA) can capture the key aspects of the Anderson–Mott localization. Our main focus will be on presenting models employing parametrized Hamiltonians, and on showing their capabilities and limitations *vis à vis* experimental results.

As discussed above, various experiments imply consistently that the Mn ions are in the high spin 2+ charge state in tetrahedrally coordinated magnetic semiconductors. Accordingly, the Mn ions are electrically neutral in II–VI compounds but act as effective mass acceptors in III–V semiconductors. It is now well established that in the absence of free carriers the dominant exchange mechanism is the short-range superexchange in zinc-blende magnetic semiconductors. This mechanism leads to antiferromagnetic interactions, except perhaps for some Cr- and V-based compounds, for which the presence of a ferromagnetic coupling is theoretically predicted [74, 75]. Remarkably, owing to the large exchange energy $|\beta N_0|$ and the high density of states, the hole-mediated long-range ferromagnetic exchange interaction can overcome antiferromagnetic superexchange [26]. Indeed, as already emphasized, the presence of holes is essential for the existence of the ferromagnetic order in Mn-based semiconductors. Furthermore, the relevant spin–spin interaction is long range according to neutron studies [76].

It should be recalled at this point that electronic states in doped semiconductors undergo dramatic changes as a function of the impurity concentration [77, 78]. Hence, the hole states, and possibly hole-mediated exchange mechanisms, may *a priori* undergo dramatic changes as function of the Mn content $x$ and the concentrations of acceptors $N_A$ and compensating donors $N_D$. The evolution of electronic states in doped semiconductors is governed by the ratio of the average distance between the carriers $r_c$ to the effective impurity Bohr radius $a_B$, determined by both Coulomb field and short-range potential of equation (1). In the case of the holes in (Ga,Mn)As,

$r_c = (3/4\pi p)^{1/3}$, $p = xN_0 - N_D$, and $a_B \approx 0.78$ nm [72]. A similar value is expected for (Zn,Mn)Te containing nitrogen acceptors [16]. However, as already mentioned, the p–d interaction may significantly contribute to the impurity binding energy and diminish the effective Bohr radius. In the range of small impurity concentrations, $r_c \gg a_B$, the holes are tightly bound to acceptors. Hence, the conductivity vanishes in the limit of zero temperature. At non-zero temperatures, the charge transport proceeds either via phonon-assisted hopping between occupied and empty acceptors or by means of thermal activation from the acceptor levels to the valence band. In a pioneering work Pashitskii and Ryabchenko [79] evaluated the strength of exchange interactions between localized spins mediated by band carriers thermally activated from impurity levels. More recently, Wolff *et al* [80] considered carriers localized on impurities and forming bound magnetic polarons (BMP). It was found that there exists a range of parameters, in which the coupling between the BMP is ferromagnetic. This idea was further explored by Bhatt and Wan [81], who examined by Monte Carlo simulations properties of a ferromagnetic phase transition driven by the interactions between the BMP. In a more recent work Berciu and Bhatt [72] discuss, within the MFA, ferromagnetic interactions mediated by quantum hopping of holes within the Mn acceptor impurity band in III–V materials. The compensation is taken into account by assuming that the number of the holes is smaller than that of the Mn sites, but no effects of ionized donors on the site energies is taken into account. An important result is that the disorder in impurity positions tends to *enhance* the magnitude of $T_C$.

Two other groups noted that a long-range exchange interaction between Mn spins can be mediated by holes undergoing quantum hoping from the Mn-derived impurity states to the extended valence band states. Inoue *et al* [82] adopted the Slater–Koster approach, well known in the physics of resonant states, for the case of two magnetic impurities. It has been found, by a model calculation, that the pairs of Mn spins coupled to the valence band states have a lower energy in the ferromagnetic than in the antiferromagnetic configuration. Litvinov and Dugayev [83] suggested than the ferromagnetic spin–spin interaction can originate from virtual excitations between the acceptor-like impurity level and the valence band, a variant of the Bloembergen–Rowland indirect exchange mechanism. They evaluated Curie temperatures by using a formula, derived originally for excitations between valence and conduction bands, without proving its correctness for the case in question.

With the increase of the net acceptor concentration, the impurity band merges with the valence band. For $r_c \ll a_B$, the holes reside in the band, and their quasi-free propagation is only occasionally perturbed by scattering of Mn and other defect potentials, whose long-range Coulomb part is screened by the carrier liquid. Here, the celebrated Ruderman–Kittel–Kasuya–Yosida (RKKY) mechanism, driven by intraband virtual excitations, is expected to dominate. In the context of III–V magnetic semiconductors, this mechanism was discussed by Gummich and da Cunha Lima [84] and Matsukura *et al* [85]. At the same time, the present author and co-workers [26] demonstrated the equivalence of the RKKY and Zener [86, 87] models, at least on the level of the mean-field and continuous medium approximations. However, with

no doubts, beyond those approximations such equivalence can be questioned [88]. Within the Zener approach [86, 87], and its nuclear spin variant [89], the degree of spin ordering, $M_q$, at given temperature $T$ is sought by minimizing the total free energy of the spin and carrier subsystems, $F[M_q]$. Here, $M_q$ denotes the Fourier components of localized spin magnetization $M(r)$, so that the minimum of $F[M_q]$ for $M_{q=0} \neq 0$ implies the ferromagnetic order. Because of its relevance, the Zener model will be discussed in some details in a subsequent subsection.

In view of the above discussion a question arises whether the hole-mediated ferromagnetism appear in the insulator or in the metallic phase. It is well established that the metal-insulator transition (MIT) occurs at $r_c \approx 2.4a_B$ in doped non-magnetic semiconductors [90]. According to this criterion one gets the critical hole concentration $p_c = 4 \times 10^{19}$ cm$^{-3}$ for $a_B = 0.78$ nm. Experimentally, the MIT occurs at about 3.5% of Mn in (Ga,Mn)As, i.e. for $N_0x = 7 \times 10^{20}$ cm$^{-3}$ [85, 91, 92]. A large difference between these two values is presumably caused by the compensation as well as by the enhancement of localization by the sp–d exchange scattering [53], an effect observed also in p-(Zn,Mn)Te [16]. This is documented in both (Ga,Mn)As [92] and p-(Zn,Mn)Te [16] by the presence of negative magnetoresistance and the associated insulator-to-metal transition driven by the magnetic field [92]. In addition to the MIT at $x \approx 0.035$ in (Ga,Mn)As, a reentrant insulator phase is observed for $x > 0.06$ [85]. Presumably, a self-compensation mechanism is involved, such as the appearance of interstitial Mn donors, as suggested by first principles studies [93]. Further efforts are necessary to test this hypothesis and, more importantly, to push the Mn solubility limit towards higher $x$ values.

Perhaps, the most intriguing property of the materials in question is that the ferromagnetism is observed on the both sides of MIT [16, 85, 91]. It is, therefore, interesting to contemplate the nature of electronic states in the vicinity of the MIT in doped semiconductors. Obviously, the random spatial distribution of acceptor and donor centres gives rise to strong spatial fluctuations in the carrier density and states characteristics. According to the phenomenological two-fluid model there exist two kinds of relevant states [94]. The first are strongly localized and thus singly occupied states associated with the attractive potential of a single majority impurity. The strongly localized carriers barely contribute to the conduction process. However, they produce a Curie-like component in the magnetic susceptibility and give rise to the presence of BMP in magnetic semiconductors. Obviously, the impurity-like states dominate deeply in the insulating phase but their presence is noticeable also in the metallic phase [50, 94, 95]. The second pool of states determines the conductivity, so that properties of these states are described by the scaling theory of MIT. Accordingly, the corresponding localization radius $\xi$ is rather controlled by interference of multi-scattering processes than by the attractive potential of a single impurity. Thus, $\xi$ of these weakly localized states is significantly larger than $a_B$, and diverges on approaching the MIT from the insulator side. It is worth noting that such a two-fluid model is consistent with a.c. conductivity studies [96], which show the coexistence of weakly and strongly localized

states near the MIT in (Ga,Mn)As. Furthermore, the merging of impurity and band states in this range is substantiated by angle-resolved photoemission spectra in the same system [60].

In order to tell the dominant mechanism accounting for the existence of long-range spin order in ferromagnetic semiconductors it is instructive to trace the evolution of their magnetic properties on crossing the MIT. Remarkably, in contrast to rather strong changes of resistivity, the evolution of magnetic properties is gradual. This substantiates the notion that thermodynamic properties do not exhibit any critical behaviour at MIT as they are insensitive to large-scale characteristics of the wavefunctions. Importantly, the values of Curie temperature are found to grow with the degree of the material metallicity [16, 85, 97, 98]. Moreover, the examination of magnetization as a function of temperature and magnetic field indicates that virtually all Mn spins contribute to ferromagnetic order in the most metallic samples [16, 85, 91, 97, 98]. However, on crossing the MIT (by lowering $x$), the relative concentration of ferromagnetically coupled spins decreases substantially. According to XMCD results [61], about 10% of Mn spins is involved in ferromagnetism of Ga$_{1-x}$Mn$_x$As with $x = 2$%. Also ferromagnetic resonance studies [56] and direct magnetization measurements demonstrate that only a part of spins contribute to spontaneous magnetization, while the alignment process of the remaining moments occurs according to a Brillouin function for a weakly interacting spin system [91]. Remarkably, the anomalous Hall effect reveals clearly the presence of the first component but hardly points to the existence of any loose spins [16, 85].

The above findings indicate that Mn spins in the regions visited by itinerant holes are coupled ferromagnetically. These holes set long-range ferromagnetic correlation between Mn spins, including those contributing to BMP that are formed around singly occupied local states. Obviously, the ferromagnetic portion of the material, and thus the magnitude of spontaneous magnetization, grows with the dopant concentration, attaining 100% in the metallic phase. Such a trend is confirmed by the available data, as discussed above. Thus, the delocalised or weakly localized holes are responsible for ferromagnetic correlation in both (Ga,Mn)As and (Zn,Mn)Te:N [27]. At the same time, mechanisms that involve strongly localized states, such as excitations from impurity levels or a direct coupling between BMP, appear to be of lesser importance.

According to the two-fluid scenario referred to above, the BMP are present on the both sides of the metal–insulator transition (MIT) [95]. As already mentioned, the coupling between the BMP appears to be ferromagnetic [80]. Since $T_C$ is proportional to the square of spin vector length, the weight of the BMP contribution may exceed their relative concentration. To gain the Coulomb energy, the BMP are preferentially formed around close pairs of ionized acceptors. In the case of III–V materials, one hole localized at two Mn ions generates, via Zener's double exchange [70], a strong ferromagnetic coupling that overcompensates the intrinsic superexchange antiferromagnetic interaction. In contrast, in II–VI compounds, for which the acceptor cores do not carry any spin and the degree of compensation by

donors is low, BMP are not preferentially form around the Mn pairs. Accordingly, the pairs of the close Mn spins remain antiferromagnetically aligned, even in p-type samples. This diminishes the effective concentration of the Mn spins contributing to the ferromagnetic order, $x_{eff} < x$, and decreases the effective Curie-Weiss temperature by $T_{AF}$, both parameters known from magnetization studies on undoped II–VI DMS. The weakening of the ferromagnetism by the superexchange in the case of II–VI compounds, and the virtual absence of the corresponding effect in III–V materials, where $T_{AF} \approx 0$ and $x_{eff} \approx x$, constitutes the important difference between these two families of magnetic semiconductors. This fact is taken into account when evaluating the Mn contribution to the total free energy of particular systems. It is worth adding that recent Monte Carlo simulations [99] carried out starting from an impurity band model, provides an additional support for the two fluid scenario.

### 4.2. Mean-field Zener model and its limitations

In terms of the mean-field Zener model of the carrier-mediated ferromagnetic interactions [26, 87, 100, 101] the equilibrium magnetization, and thus the $T_C$ is determined by the minimum of the Ginzburg–Landau free-energy functional $F[M(r)]$ of the system, where $M(r)$ is the local magnetization of the localized spins. This is a rather versatile scheme, to which carrier correlation and confinement [15, 18, 26, 39, 101, 102], $k \cdot p$ and spin–orbit couplings [16, 27, 28, 103] as well as weak disorder and antiferromagnetic interactions [16, 18, 26] can be introduced in a controlled way, and within which the quantitative comparison of experimental and theoretical results is possible [16, 20, 28, 104]. In its general formulation, the model allows for non-uniform ground states ($M(q > 0) \neq 0$), such spin-density waves or non-collinear (canted) magnetic structures [39].

In theory developed by the present authors and co-workers [26–28], the hole contribution to $F$ is computed by diagonalizing the $6 \times 6$ Kohn–Luttinger $k \cdot p$-matrix containing the p–d exchange contribution, and by the subsequent computation of the partition function $Z$, $F_c = -k_B T \ln Z$. In the case of a strongly degenerate Fermi liquid, $-E_F|/k_B T \gg 1$, $F_c$ can be replaced by the ground state energy. However, this approximation would severely overestimate $T_C$ in materials with low hole densities or with high $T_C$ values and, therefore, has not been employed for such situations [20, 27, 28]. The model is developed for both zinc-blende and wurzite semiconductors, takes the effects of the spin–orbit interaction into account, and allows for the presence of both biaxial strain and quantizing magnetic field. The enhancement of the tendency towards ferromagnetism by the carrier–carrier exchange interactions is described by the Fermi liquid parameter $A_F$. The value $A_F = 1.2$ was evaluated within the LSDA for the 3D carrier liquid of the relevant density [101]. Importantly, the formalism has been extended by König et al [105, 106], who evaluated the dependence of the carrier free energy on the wave vector $q$. This dependence provides information on magnetic stiffness, which together with magnetic anisotropy, determine the dispersion of spin waves [106] and the structure of magnetic domains [104].

It is, of course, important to comment explicitly main approximations behind the Zener model. Obviously, this model may not be applicable to DMS containing magnetic impurities other than Mn, in which d levels reside in the band gap and correlation energy $U$ is relatively small. In the Mn-based DMS, however, the magnetic constituent appears to be well described in terms of the the Anderson impurity model and, thus, such DMS can be regarded as charge transfer insulators. This means that the spins are localized, so that the d electrons do not participate in charge transport. There exist, however, quantum fluctuations (hybridization) between the p and d orbitals, which result in the Kondo-like interaction that couples the spin and the carrier parts of the free energy. It should be emphasized that results of the LSDA computations [73] point to a rather large weight of the d electrons at the Fermi level and, hence, imply the ferromagnetism to be driven by the mechanism of double exchange. This controversy is perhaps the most intriguing open issue in theory of magnetic semiconductors.

The use of the spin, not carrier magnetization, as the order parameter in the Zener model is a consequence of the adiabatic approximation: spin dynamics is assumed to be much slower than that of the carriers. This approximation may break down if, for instance, a characteristic energy of spin–spin antiferromagnetic interactions would become greater than $T_C$. Furthermore, the order parameter can be regarded as continuous as long as the concentration of the spins is much larger than that of the holes, $x_{eff}N_0 \gg p$. Importantly, in this range, the mean-field value of the ordering temperature $T_C(q)$ deduced from the Zener and the RKKY model are identical, independently of microscopic spin distribution [26].

However, in the opposite limit, $x_{eff}N_0 < p$, important changes in the hole response function occur at the length scale of a mean distance between the localized spins. Accordingly, the description of spin magnetization by the continuous-medium approximation, which constitutes the basis of the Zener model, ceases to be valid. In contrast, the RKKY model is a good starting point in this regime [16], as it provides the dependence of the interaction energy of particular spin pairs as a function of their distance. This makes it possible to evaluate the system energy for a given distribution of the localized spins. The resulting competition between the ferromagnetic and antiferromagnetic interactions is expected to grow with $p/x_{eff}N_0$, and may lead, through non-collinear (canted) spin arrangement [107, 108], to the spin-glass phase [109]. Alternatively, with decreasing $x$ at given $p$, the Kondo effect may show up [26].

It is interesting to note that the role of thermodynamic fluctuations of magnetization, that is the inaccuracy of the mean-field approximation (MFA), grows also with $p/x_{eff}N_0$. It is well known that the MFA results are exact, also in low-dimensional systems, if the range of ferromagnetic interactions is infinite [110]. The decay of the strength of the carrier-mediated exchange interaction with the distance $r$ between two Mn spins is described by the RKKY oscillatory function. At small $r$, the interaction is ferromagnetic, and then changes sign at $r = 1.2r_c$, where $r_c$ is an average distance between the carriers that mediate the spin–spin coupling. This implies that the MFA is valid quantitatively at $p \ll x_{eff}N_0$, a conclusion consistent with the estimate of $T_C$ taking the spin

wave excitations into account [105]. Actually, however, the range of validity of the MFA is significantly larger [107] than that initially proposed [105, 111], as the magnitudes of spin stiffness evaluated within the $6 \times 6$ Luttinger model is much greater [106] than those obtained for a simple parabolic band [105]. The dynamic mean-field approach [112] and, especially, hybrid Monte-Carlo algorithms [113] have potential to sheet some light on ferromagnetism in the regime beyond the validity of the MFA.

Finally, we address the question about the role played by disorder. Since thermodynamic properties of the carrier liquid are relatively weakly perturbed by scattering, its effect on the hole-mediated ferromagnetism can be neglected to a first approximation. When disorder grows and the MIT is approached, the mean free path becomes comparable to the inverse Fermi wave vector. Within the Zener model, the effect of the finite mean free path $l_e$ can be described by scattering broadening of the density of states [18, 26], which reduces $T_C$. Technically, this follows from the averaging of the free energy over possible impurity distributions. Equivalently, diffusive character of carrier transport leads to exponential dumping of the RKKY interactions at distances longer than $l_e$. However, large fluctuations in the carrier distribution have to be taken into account at criticality and on the insulator side of the MIT. As already argued, the magnetization is small in areas which are not visited by the carriers, whereas its magnitude is large there, where delocalized or weakly localized carriers reside. Remarkably, this enhances $T_C$ over the value expected for the average carrier density [72] but reduces the magnitude of sample-average spontaneous magnetization [16, 27, 28]. The interplay between Anderson–Mott localization, Stoner magnetism, and carrier-mediated spin–spin interaction is certainly an appealing area for future research. Recent theoretical works in this direction are indeed encouraging [114].

## 5. Comparison of the Zener model to selected experimental results

### 5.1. Magnetic circular dichroism in (Ga,Mn)As

Within the Zener model, the strength of the ferromagnetic spin–spin interaction is controlled by the $k \cdot p$ parameters of the host semiconductor and by the magnitude of the spin-dependent coupling between the effective mass carriers and localized spins. In the case of II–VI DMS, detailed information on the exchange-induced spin-splitting of the bands, and thus on the coupling between the effective mass electrons and the localized spins has been obtained from magnetooptical studies [52, 53]. A similar work on (Ga,Mn)As [116–118] led to a number of surprises. The most striking was the opposite order of the absorption edges corresponding to the two circular photon polarizations in (Ga,Mn)As comparing to II–VI materials. This behaviour of circular magnetic dichroism (MCD) suggested the opposite order of the exchange-split spin subbands, and thus a different origin of the sp–d interaction in these two families of DMS. A new light on the issue was shed by studies of photoluminescence (PL) and its excitation spectra (PLE) in p-type (Cd,Mn)Te quantum wells
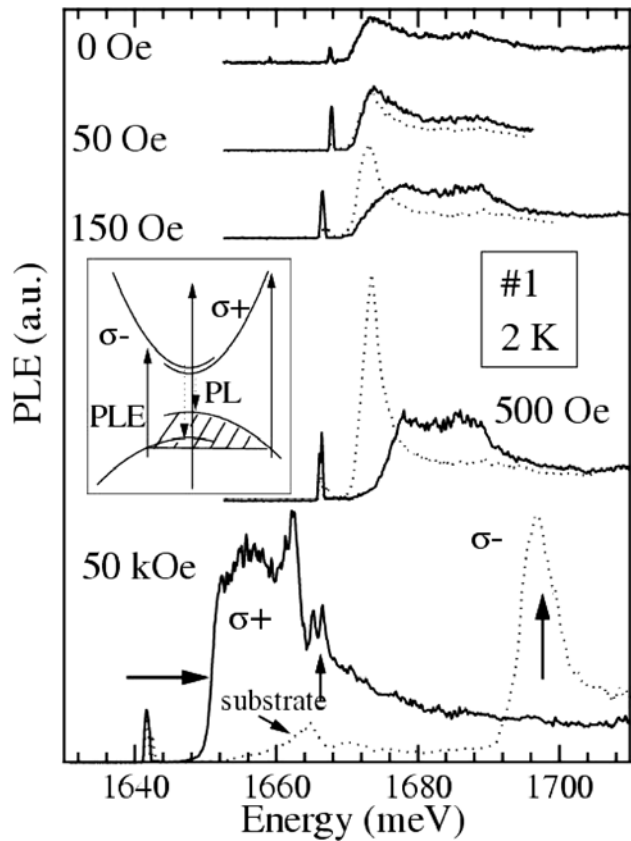


**Figure 3.** Photoluminescence excitation spectra (PLE), that is the photoluminescence (PL) intensity as a function of the excitation photon energy intensity, for $\sigma^+$ (solid lines) and $\sigma^-$ (dotted lines) circular polarizations at selected values of the magnetic field in a modulation-doped p-type quantum well of $Cd_{0.976}Mn_{0.024}Te$ at 2 K. The photoluminescence was collected in $\sigma^+$ polarization at energies marked by the narrowest features. The sharp maximum (vertical arrow) and step-like form (horizontal arrow) correspond to quasi-free exciton and transitions starting at the Fermi level, respectively. Note reverse ordering of transition energies at $\sigma^+$ and $\sigma^-$ for PL and PLE (the latter is equivalent to optical absorption). The band arrangement at 150 Oe is sketched in the inset (after [15]).

[15]. As shown schematically in figure 3, the reversal of the order of PLE edges corresponding to the two circular polarizations results from the Moss–Burstein effect, that is from the shifts of the absorption edges associated with the empty portion of the valence subbands in the p-type material. This model was subsequently applied to interpret qualitatively the magnetoabsorption data for metallic (Ga,Mn)As [117]. More recently, the theory was extended by taking into account the effect of scattering-induced mixing of $k$ states [58]. As shown in figure 4, this approach explains the slop of the absorption edge as well as its field-induced splitting assuming the value of the p–d exchange energy $\beta N_0 = -1$ eV.

Surprisingly, however, the anomalous sign of the MCD was present also in non-metallic (Ga,Mn)As, in which EPR signal from occupied Mn acceptors was seen [56]. It has, therefore, been suggested that the exchange interaction between photo- and bound-holes is responsible for the anomalous sign of the MCD in those cases [117]. The presence of such a strong exchange mechanism is rather puzzling, and it
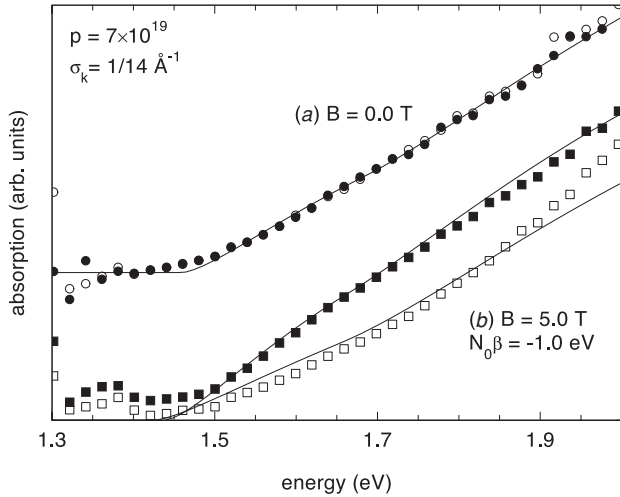
**Figure 4.** Transmission of $Ga_{0.968}Mn_{0.032}As$ film for two circular light polarizations in the Faraday configuration in the absence of the magnetic field (data shifted up for clarity) and in 5 T at 2 K (points) [117]. Solid lines are calculated for the hole concentration $p = 7 \times 10^{19}$ cm$^{-3}$, exchange energy $N_0\beta = -1$ eV, and allowing for scattering-induced breaking of the $k$ selection rules [58].

should be seen in non-magnetic p-type semiconductors. At the same time, according to our two-fluid model, the co-existence of strongly and weakly localized holes is actually expected on the both sides of the MIT. Since the Moss–Burstein effect operates for interband optical transitions involving weakly localized states, it leads to the sign reversal of the MCD, also on the insulating side of the MIT.

Another striking property of the MCD is a different temperature dependence of the normalized MCD at low and high photon energies in ferromagnetic (Ga,Mn)As [118]. This observation was taken as an evidence for the presence of two spectrally distinct contributions to optical absorption [118]. A quantitative computation of MCD spectra has recently been undertaken [28]. The theoretical results demonstrate that because of the Moss–Burstein effect, the magnetization-induced splitting of the bands leads to a large energy difference between the positions of the absorption edges corresponding to the two opposite circular polarizations. This causes an unusual dependence of the low-energy onset of MCD on magnetization, and thus on temperature. These considerations lead to a quantitative agreement with the experimental findings, provided that the actual hole dispersion and wavefunctions are taken for the computation of MCD.

In conclusion, a.c. conductivity in the far infrared [96] as well as to photoemission [59, 60] and XMCD [61, 62] in the range of high photon energies, together with magnetooptical characteristics discussed here, are consistent with the picture of electronic states advocated for (Ga,Mn)As in the previous section. In particular, (Ga,Mn)As exhibits properties generic to doped semiconductors in the vicinity of the metal–insulator transition. Furthermore, no experimental results have so far been collected in favour of the valence band splitting corresponding to the p–d exchange integral as high as $\beta N_0 \approx -4$ eV, as suggested by *ab initio* computations within the LSDA [73].

## 5.2. Curie temperature and spontaneous magnetization in p-type and n-type Mn-based DMS

In order to compare theoretical expectations concerning $T_C$ to experimental results, it is convenient to introduce the normalized ferromagnetic temperature $T_F/x_{eff} = (T_C + T_{AF})/x_{eff}$ which, within the mean-field Zener model, should not depend on the Mn concentration $x$. We recall that $x_{eff} < x$ and $T_{AF} > 0$ take into account the presence of antiferromagnetic exchange interaction in II–VI DMS. Figure 5 presents $T_F/x_{eff}$ for $Ga_{1-x}Mn_xAs$ [14, 85, 119], p-$Zn_{1-x}Mn_xTe$ [16, 120], and quantum wells of p-$Cd_{1-x}Mn_xTe$ [18, 33] as a function the Fermi wavevector determined from the value of the hole concentration $p$ assuming the Fermi sphere to be isotropic. The hole concentration was deduced either from the Hall resistance [16, 119] or from the Moss–Burstein shift [18, 20]. We have to emphasize that because of a contribution from the anomalous (spin) Hall effect and a non-uniform hole distribution in thin layers, the evaluation of the hole concentration is by no means straightforward in magnetic semiconductors.

A number of important conclusions emerges from the comparison of experimental and theoretical results. First, the theory [27, 28] with $\beta N_0 = -1.2$ eV [59] explains the large magnitude of $T_C = 110$ K [14, 85] for $Ga_{0.947}Mn_{0.053}As$ containing $3.5 \times 10^{20}$ holes per cm$^3$ [119]. Second, in contrast to Mn-based III–V DMS, it is essential—in the case of II–VI materials—to take into account the presence of magnetically inert nearest-neighbour Mn pairs. Such pairs not only diminish the effective Mn concentration but also make the antiferromagnetic portion of the RKKY interaction become more significant. This results in lowering $T_C$ at large $p$ (dotted line) [16]. Third, scaling theory of electronic states near the MIT, discussed in the previous section, makes it possible to explain the presence of ferromagnetism on the both sides of the MIT, and a non-critical evolution of $T_C$ across the critical point, a behaviour observed in both (Ga,Mn)As [85] and p-(Zn,Mn)Te [16, 120, 121]. Importantly, in agreement with this scenario, a ferromagnetic component of the material increases with the hole concentration [16]. However, as already explained, because of RKKY oscillations, the present theory (solid lines) overestimates the magnitude of $T_C$ if the hole and Mn concentrations becomes comparable, $p \approx x_{eff}N_0$. In contrast, the actual value of $T_C$ can be larger than that of figure 5 on the insulator side of the MIT because of the fluctuations in the carrier density and a non-linear contribution of spin clusters within the BMP. This might be the reason for a relatively high values of $T_C$ detected recently in (In,Mn)As [122]. Last but not least, according to figure 5, in modulation doped (Cd,Mn)Te/(Cd,Mg,Zn)Te:N heterostructures, due to the enhanced density-of-states (DOS) at low energies in 2D systems and reduced localization by the distant nitrogen acceptors, the ferromagnetic transition occurs even for the densities of the hole liquid as low as $10^{17}$ cm$^{-3}$ [15, 18]. The present theory describes correctly the dependence of $T_C$ on $x$ and $p$, provided that the exchange interaction between the holes and disorder broadening of DOS are taken into account [18, 20].

Two effects appear to account for the greater $T_C$ values in p-(Ga,Mn)As than in p-(Zn,Mn)Te at given $p$ and $x$. First is the smaller magnitude of the spin–orbit splitting between the
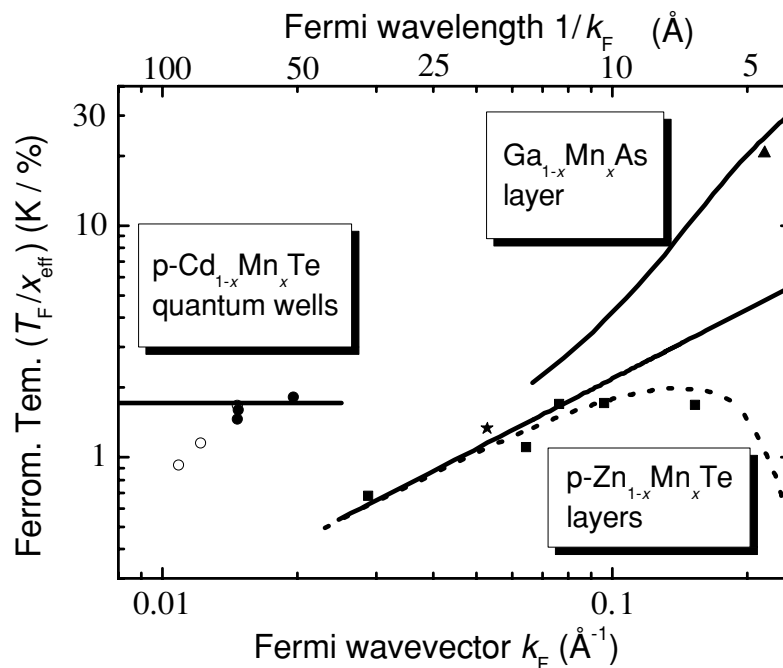
**Figure 5.** Experimental (symbols) and calculated (lines) normalized ferromagnetic temperature, $T_F/10^2 x_{eff}$, versus the wave vector at the Fermi level for $Ga_{1-x}Mn_xAs$ (triangle) [85, 119], $Zn_{1-x}Mn_xTe:N$ (squares) [16, 120], $Zn_{1-x}Mn_xTe:P$ (star) [120], and quantum well of p-$Cd_{1-x}Mn_xTe$ (circles) [18, 33]. Solid lines: Zener and $6 \times 6$ Luttinger model for the 3D [28] and 2D case [26]; dotted line: the RKKY and $6 \times 6$ Luttinger model for $x_{eff} = 0.015$, taking into account the effect of the antiferromagnetic interactions on statistical distribution of unpaired Mn spins [16].

$\Gamma_8$ and $\Gamma_7$ bands in arsenides, $\Delta_o = 0.34$ eV, in comparison to that of tellurides, $\Delta_o = 0.91$ eV. Once the Fermi energy $E_F$ approaches the $\Gamma_7$ band, the density-of-states effective mass increases, and the reduction of the carrier spin susceptibility by the spin–orbit interaction is diminished. The computed value of $T_C$ for $p = 3 \times 10^{20}$ cm$^{-3}$ is greater by a factor of 4 in (Ga,Mn)As than that evaluated in the limit $\Delta_o \gg E_F$. The other difference between the two materials is the destructive effect of antiferromagnetic interactions, which operate in II–VI compounds but are of minor importance in III–V materials, as argued in the previous section.

Since in semiconductors the magnitude of exchange splitting of bands is comparable to the Fermi energy, the growth of spontaneous magnetization $M_s$ on lowering temperature deviates from the Brillouin-type behaviour even in the mean-field approximation [15, 16, 18, 26, 28]. Because of extremely low hole densities, the effect is particularly well visible in the case of modulation-doped (Cd,Mn)Te/(Cd,Mg,Zn)Te:N heterostructures [15, 18]. Furthermore, the contribution from carrier magnetic moments and disorder-induced fluctuations in the carrier distribution constitute other sources of corrections to the Brillouin-type dependence. However, with the increase of the hole concentration, $M_s(T)$ evaluated within the mean-field Zener model tends toward the Brillouin function for material parameters of (Ga,Mn)As [28], an expectation corroborated by the experimental results [85, 98].

Finally, we turn to materials, in which the Fermi level resides in the s-type conduction band. Because of small s–d exchange energy and low density of states, no ferromagnetism

is expected above 1 K in such a case [26]. Experimental results for n-(In,Mn)As [123], (Ga,Mn)As:Sn [124], and (Zn,Mn)O:Al [120] confirm this expectation. With this in mind, the presence of indications of ferromagnetism in n-type (Ga,Mn)N [125] is challenging.

### 5.3. Effects of strain

Both hydrostatic and axial strain affect the valence band, and thus alter the magnitude of the density of states and $T_C$. Quantitatively, however, the effect is evaluated to be small [28]. There exists another mechanism by which strain may affect $T_C$. It is presently well known that the upper limit of the achievable carrier concentration is controlled by pinning of the Fermi level by impurity or defect states in virtually all compound semiconductors. Since the energies of such states in respect to bands vary strongly with the bond length, the hole concentration and thus $T_C$ will depend on strain.

Apart from $T_C$ and spontaneous magnetization $M_s$, it is interesting to consider means making it possible to tailor magnetic anisotropy, and thus the direction of the spontaneous magnetization, the coercive force, the switching field, the domain structure. Already early studies of the ferromagnetic phase in $In_{1-x}Mn_xAs$ [126] and $Ga_{1-x}Mn_xAs$ [127, 128] demonstrated the existence of sizable magnetic anisotropy. Magnetic anisotropy is usually associated with the interaction between spin and orbital degrees of freedom of the d-electrons. According to the model advocated here, these electrons are in the $d^5$ configuration. For such a case the orbital momentum $L = 0$, so that effects stemming from the spin–orbit coupling are expected to be rather weak. It has, however, been noted

that the interaction between the localized spins is mediated by the holes that have a non-zero orbital momentum [27]. An important aspect of the Zener model is that it does take into account the anisotropy of the carrier-mediated exchange interaction associated with the spin–orbit coupling in the host material [27, 28, 103], an effect difficult to include within the standard approach to the RKKY interaction [108].

A detail numerical analysis of anisotropy energies has been carried out for a number of experimentally important cases [27, 28, 103]. In particular, the cubic anisotropy as well as uniaxial anisotropy under biaxial strain have been studied as a function of the hole concentration $p$. The computation indicates that for the parameters of $Ga_{1-x}Mn_xAs$ films grown along the [001] direction, the spontaneous magnetization $M$ lies in the (001) plane, and the easy axis is directed along [100] or along [110] (or equivalent) crystal axis depending on the degree of the occupation the hole subbands as well as on their mixing by the p–d and $k \cdot p$ interactions. As a result, the easy axis fluctuates between [100] and [110] as a function of $p$, the preferred direction for typical hole concentrations being [110]. The magnitude of the external magnetic field $H_{cu}$ that aligns $M$ along the hard direction in the (001) plane is evaluated to be up to 0.2 T [28]. Since, however, the orientation of the easy axis changes rapidly with $p$ and $M$, disorder—which leads to broadening of hole subbands—will presumably diminish the actual magnitude of magnetic anisotropy. The field $\mu_o H_{cu}$ determines also the magnitude of the switching field, which could be observed in microstructures containing only a single domain. In macroscopic films, however, smaller values of the coercive field $\mu_o H_c$ are expected as actually observed: typically $\mu_o H_c = 4\,mT$ for the magnetic field along the easy axis in the (001) plane in $Ga_{1-x}Mn_xAs$ [128].

It can be expected that strain engineering can efficiently control magnetic properties resulting from the hole-mediated exchange. Indeed, sizable lattice-mismatch driven by biaxial strain is known to exist in semiconductor layers. In some cases, particularly if epitaxy occurs at appropriately low temperatures, such strain can persist even beyond the critical thickness due to relatively high barriers for the formation of misfit dislocations. It has been found that the biaxial strain leads to uniaxial anisotropy, whose magnitude can be much greater than that resulting from either cubic anisotropy or stray fields. As shown in figure 6, for the experimentally relevant values of $p$ and $M$, the easy axis is predicted to be oriented along [001] direction for the tensile strain, whereas it should reside in the (001) plane for the case of unstrained or compressively strained films [27, 28, 103]. This is corroborated by the experimental study [127, 128], in which either (In,Ga)As or GaAs substrate was employed to impose tensile or compressive strain in $Ga_{1-x}Mn_xAs$, respectively. In particular, for the $Ga_{0.965}Mn_{0.035}As$ film on GaAs, for which $\epsilon_{xx} = -0.24\%$, the anisotropy field $\mu_o H_{un} = 0.4 \pm 0.1\,T$ is observed [127, 128], in quantitative agreement with the theoretical results of figure 6. This field is about two orders of magnitude greater than that evaluated from the extrapolation of ESR data on single-ion anisotropy at low $x$ [129], a result confirming the dominant contribution of the holes to the magnitude of $H_{un}$. Though no theoretical computations have been performed for $In_{1-x}Mn_xAs$, the qualitatively similar effect of biaxial strain is expected, in agreement with the early experimental results [126].

It worth noting that similarly to strain, also confinement of the holes affects the magnetic anisotropy—in accord with the theoretical model, the easy axis is oriented along the growth direction in the ferromagnetic p-(Cd,Mn)Te quantum wells [15, 18].

### 5.4. Domain structure

Recently, the structure of magnetic domains in $Ga_{1-x}Mn_xAs$ under tensile strain has been determined by micro-Hall probe imaging [130]. The regions with magnetization oriented along the [001] and [00] easy axis form alternating stripes extending in the [110] direction. This indicates, for either Bloch or Néel domain walls, that the in-plane easy axis is rather along [110] than along [100] directions, a conclusion consistent with the theoretical expectation for in-plane (cubic) magnetic anisotropy presented above. As shown in figure 7, the experimentally determined stripe width is $W = 1.5\,\mu m$ at 5 K for 0.2 $\mu m$ film of $Ga_{0.957}Mn_{0.043}As$ on $Ga_{0.84}In_{0.16}As$, for which tensile strain of $\epsilon_{xx} = 0.9\%$ is expected.

According to micromagnetic theory [131], $W$ is determined by the dimensionless parameter $\lambda_c$, which is given by the ratio of the domain wall and stray field energies. The former is proportional to $M^2$, whereas the latter scales with the product of anisotropy energy $K_u$ [28, 103] and magnetic stiffness $A$ [106]. Figure 7 presents the calculated values of $W(T)$ [104] in comparison to the experimental data for (Ga,Mn)As [130]. The material parameters collected in [28], and employed to generate theoretical results of figures 5 and 6, have been adopted. Furthermore, in order to establish the sensitivity of the theoretical results to the parameter values, the results calculated for a value of $\lambda_c$ 1.8 times larger are included as well. The computed value for low temperatures, $W = 1.1\,\mu m$, compares favourably with the experimental finding, $W = 1.5\,\mu m$. However, the model predicts much weaker temperature dependence of the domain width $W$ than observed experimentally, which are linked [104] to critical fluctuations, disregarded in the mean-field approach.

## 6. Towards high-temperature ferromagnetic semiconductors

### 6.1. Mn-based tetrahedrally coordinated DMS

In view of the general agreement between experiment and theory for $T_C$ and the magnetic anisotropy, it is tempting to extend the model for material systems that might be suitable for fabrication of functional ferromagnetic semiconductors. For instance, the model suggests immediately that $T_C$ values above 300 K could be achieved in $Ga_{0.9}Mn_{0.1}As$, if such a large value of $x$ would be accompanied by a corresponding increase in the hole concentration. Figure 8 presents the values of $T_C$ computed for various tetrahedrally coordinated semiconductors containing 5% of Mn per cation and $3.5 \times 10^{20}$ holes per $cm^3$ [27]. In addition to adopting the tabulated values of the band structure parameters, the same value of $\beta = \beta[Ga_{1-x}Mn_xAs]$ for all group IV and III–V compounds was assumed, which results in an increase of $|\beta N_0| \sim a_o^{-3}$, where $a_o$ is the lattice constant, a trend known to be obeyed
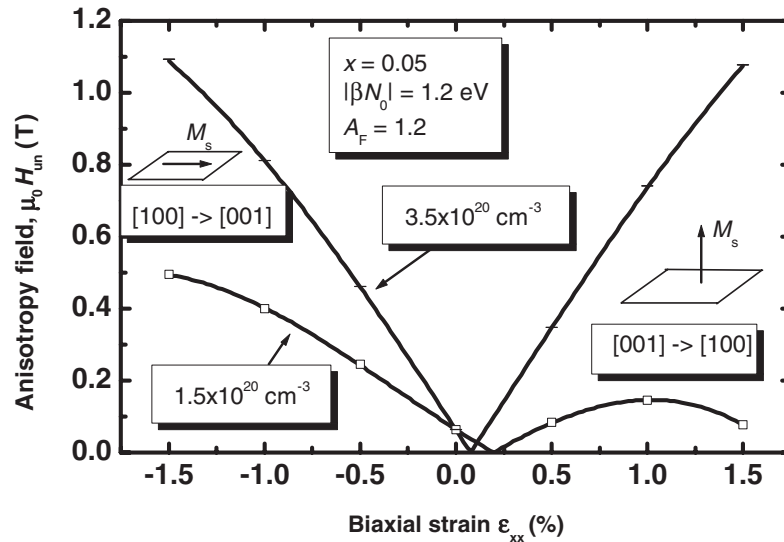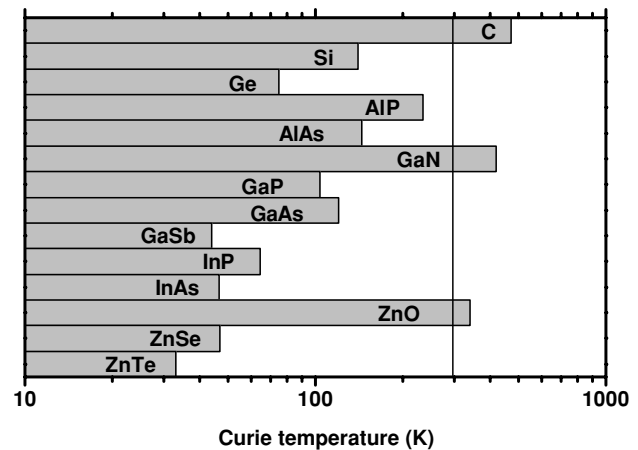
**Figure 6.** Computed minimum magnetic field $H_{un}$ necessary to align the saturation value of magnetization $M_s$ along the hard axis as a function of biaxial strain component $\epsilon_{xx}$ for two values of the hole concentrations in $Ga_{0.95}Mn_{0.05}As$ [28]. The symbol $[100] \rightarrow [001]$ means that the easy axis is along [100], so that $H_{un}$ is applied along [001].
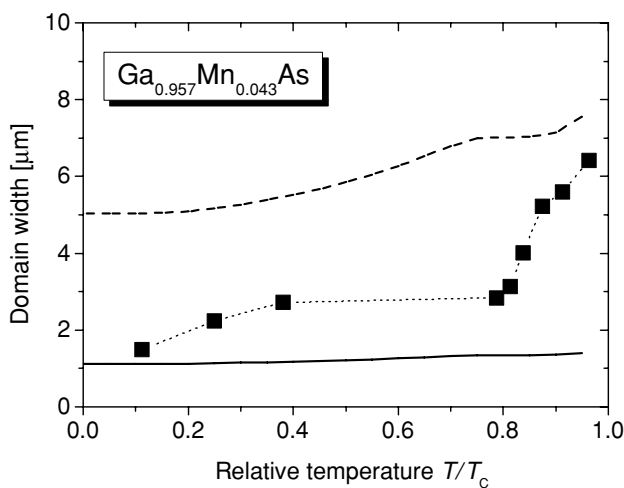


**Figure 7.** Temperature dependence of the width of domain stripes as measured for the $Ga_{0.957}Mn_{0.043}As$ film with the easy axis along the growth direction (full squares) [130]. Computed domain width is shown by the solid line. The dashed line is computed assuming that the parameter $\lambda_c$ (the ratio of the domain wall and stray field energies) is by a factor of 1.8 greater [104].



**Figure 8.** Computed values of the Curie temperature $T_C$ for various p-type semiconductors containing 5% of Mn per cation (2.5% per atom) and $3.5 \times 10^{20}$ holes per $cm^3$ (after [27, 28]).

within the II–VI family of magnetic semiconductors. For the employed parameters, the magnitude of $T_C$ for the cubic GaN is by 6% greater than that computed for the wurzite structure.

The data (figure 8) demonstrate that there is much room for a further increase of $T_C$ in p-type magnetic semiconductors. In particular, a general tendency for greater $T_C$ values in the case of lighter elements stems from the corresponding increase in p–d hybridization and the reduction of the spin–orbit coupling. It can be expected that this tendency is not altered by the uncertainties in the values of the relevant parameters. Indeed, the results of figure 8 have triggered a considerable fabrication effort, which is bringing a number of striking developments.

In particular $Ge_{1-x}Mn_x$ was found to be p-type and to exhibit $T_C$ in the excess of 100 K [132]. An even higher magnitude of $T_C$, in excess of 200 K, was found in (Ga,Mn)P:C [133], a value consistent with the prediction of figure 8 [27, 28] for the employed Mn content $x = 9.4\%$ [133]. Moreover, there are indications of ferromagnetism in (Ga,Mn)N [134–137], in some cases with $T_C$ near or above 300 K [135–137]. While further experimental work is needed to elucidate a possible role of precipitates of various Mn–Ga and Mn–N compounds, the highest value suggested up to now, $T_C = 940\,K$ for $Ga_{0.91}Mn_{0.09}N$ [136], is consistent with the expectations of the mean-field Zener model [49]. In more general terms, within this model, large magnitudes of $T_C$ result from the combined effect of the large on-site p–d exchange interaction and the efficient transfer of spin information owing to a relatively large radius of the p-like wavefunctions.

Another way investigated recently consists of searching for the high temperature ferromagnetism in compounds containing combination of elements from both II–VI and III–V materials. Layered $Ga_{1-x}Mn_xSe$ [138] and particularly chalcopyrite $Cd_{1-x}Mn_xGeP_2$ [139] are starting to provide encouraging results. Since, in general, III–V compounds can easier be doped by impurities that are electrically active, whereas II–VI materials support greater concentration of transition metals, a suggestion has been put forward to grow magnetic III–V/II–VI short period superlattice [140], in which a charge transfer to the magnetic layers will increase $T_C$.

### 6.2. Beyond Mn-based compounds

The highest spin and the associated large magnitude of the on-site correlation energy $U$ account for the divalent character of the Mn atoms in a large variety of environments. This results, in particular, in a large solubility of Mn in II–VI materials and its acceptor character in III–V compounds. A question arises about ferromagnetic properties of semiconductors containing other magnetic components. Quite generally, carrier-mediated exchange mechanism is efficient if both concentration of holes and p–d exchange energy $\beta N_0$ are appropriately large. According to figure 1, for many transition metals and hosts, the $d$ states lie in the gap. Hence, to trigger carrier-mediated exchange interactions, co-doping by shallow impurities is necessary. However, shallow acceptors will produce band holes only if the $d^{N+1}/d^N$ donor level resides at lower energies, that is in the valence band. Furthermore, except for some resonant situations, the magnitudes of $|\beta N_0|$ are small for $N < 5$ because of opposite signs of two relevant contributions [141]. With these arguments in mind, (Ga,Fe)N and (Ga,Co)N co-doped with acceptor impurities appear as promising materials [43, 68].

There are, however, other possible roads to high temperature ferromagnetism. Since for configurations other than $d^5$, the magnitude of $U$ is relatively small, the Hubbard–Mott transition, and the associated ferromagnetism may appear at increasing density of the magnetic constituent. To our knowledge no such effects have so far been detected in materials in question. Furthermore, for some magnetic ions and hosts, either $d^N/d^{N+1}$ or $d^N/d^{N-1}$ level lies below the expected energy of shallow donor or above energy of shallow acceptor, respectively. In such a situation, the co-doping by shallow impurities will rather affect the occupancy of the d levels than introduce carriers into the bands, a known semi-insulating character of semiconductors containing specific transition metals. At appropriately large concentrations of both magnetic ions and additional impurities, the carriers trapped on d levels may start to transfer, via Zener's double exchange mechanism [70], magnetic information between localized spins. Indications of ferromagnetism in the vicinity of room temperature discovered in n-(Zn,Co)O [142] and n-(Zn,V)O [143] may represent, according to figure 1, such a case. Actually, a simultaneous doping by two different magnetic impurities may serve to control both spin and charge states as well as the carrier concentration in the specific bands.

The room-temperature ferromagnetism detected after doping a few per cent of Co to nonmagnetic $TiO_2$ [144] may belong to this category. In particular, the hybridized d levels of Ti and Co may constitute the efficient channel for transmission of magnetic information between the Co spins.

Finally, one should recall the existence of, e.g., ferromagnetic europium chalcogenides and chromium spinels. In those compounds, ferromagnetism is not mediated by carrier transport. With no doubt, the availability of intrinsic and n-type tetrahedrally-coordinated ferromagnetic compounds would enlarge considerably the impact of semiconductor electronics. Actually, a theoretical suggestion has been made [74, 75] that superexchange in Cr-based and V-based II–VI compounds can lead to a ferromagnetic order. Desired material properties, such as divergent magnetic susceptibility and spontaneous magnetization, can also be achieved in the case of a strong antiferromagnetic super-exchange interaction. The idea here [145] is to synthesize a ferrimagnetic system that would consist of antiferromagnetically coupled alternating layers containing different magnetic cations, e.g., Mn and Co.

It is also tempting to consider the performance of DMS containing ions from other groups of magnetic elements. Current works on $Si_{1-x}Ce_x$ [146] and on the insulator-to-metal transition in amorphous $Si_{1-x}Gd_x$ [147] alloys can be quoted in this context. However, because of a weak hybridization between 4f and band states (exploited in Er-doped emitters), no high-temperature ferromagnetism is expected in rare-earth-based systems. More promising in this respect are materials containing 4d or 5f ions—there exists already a preliminary report on spin–spin interactions in undoped $Pb_{1-x}U_xTe$ [148]. Actually, in view of indications of room-temperature weak ferromagnetism in $(Ca,La)B_6$ [149] and polymerized rh-$C_{60}$ [150], which are built up of non-magnetic constituents, the spectrum of possibilities seems unlimited.

The above list of achievements and prospects clearly shows that searches for high temperature ferromagnetic semiconductors have evolved into a broad field of materials science. In addition to work on design and synthesis of new systems, a considerable effort will certainly be devoted to control contributions from ferromagnetic or ferrimagnetic precipitates and inclusions in the materials available already now. On theoretical side, the interplay between Anderson–Mott localization, disordered Stoner magnetism, and carrier-mediated ferromagnetism will attract a considerable attention. With no doubt we will witness many unforeseen developments in the field of ferromagnetic semiconductors in the years to come.

## Acknowledgments

# References

[1] De Boeck J *Semicond. Sci. Technol.* **17** 342 and references therein
[2] Golovach V N and Loss D 2002 *Semicond. Sci. Technol.* **17** 355 and references therein
[3] Tanaka M 2002 *Semicond. Sci. Technol.* **17** 327 and references therein
[4] Akinaga H 2002 *Semicond. Sci. Technol.* **17** 322 and references therein
[5] Johnson M 2002 *Semicond. Sci. Technol.* **17** 298 and references therein
[6] Craik D J 1975 *Magnetic Oxides* (New York: Wiley)
[7] Kasuya T and Yanase A 1968 *Rev. Mod. Phys.* **40** 684
[8] Methfessel S and Mattis D C 1968 *Encyclopedia of Physics, Magnetism, Magnetic Semiconductors* vol XVIII/1 (Berlin: Springer) pp 389–562
[9] Wachter P 1979 *Handbook on the Physics and Chemistry of Rare Earth* vol 1 (Amsterdam: North-Holland) p 507
[10] Nagaev E L 1983 *Physics of Magnetic Semiconductors* (Moscow: Mir)
[11] Mauger A and Gotard C 1986 *Phys. Rep.* **141** 51
[12] Story T 1997 *Acta Phys. Polon.* A **91** 173
[13] Ohno H, Munekata H, Penney T, von Molnàr S and Chang L L 1992 *Phys. Rev. Lett.* **68** 2664
[14] Ohno H, Shen A, Matsukura F, Oiwa A, Endo A, Katsumoto S and Iye Y 1996 *Appl. Phys. Lett.* **69** 363
[15] Haury A, Wasiela A, Arnoult A, Cibert J, Tatarenko S, Dietl T and Merle d'Aubigné Y 1997 *Phys. Rev. Lett.* **79** 511
[16] Ferrand D *et al* 2001 *Phys. Rev.* B **63** 085 201
[17] Koshihara S, Oiwa A, Hirasawa M, Katsumoto S, Iye Y, Urano C, Takagi H and Munekata H 1997 *Phys. Rev. Lett.* **78** 4617
[18] Kossacki P *et al* 2000 *Physica* E **6** 709
[19] Ohno H, Chiba D, Matsukura F, Omiya T, Abe E, Dietl T, Ohno Y and Ohtani K 2000 *Nature* **408** 944
[20] Boukari H, Kossacki P, Bertolini M, Cibert J, Tatarenko S, Ferrand D, Wasiela A, Gaj J A and Dietl T 2001 webpage http://arXivorg/abs/cond-mat/0111511
[21] Ohno Y, Young D K, Beschoten B, Matsukura F, Ohno H and Awschalom D D 1999 *Nature* **402** 790
[22] Chiba D, Akiba N, Matsukura F, Ohno Y and Ohno H 2000 *Appl. Phys. Lett.* **77** 1873
[23] Szuszkiewicz W, Dynowska E, Hennion B, Ott F, Jouanne M, Morhange J-F, Karlsteen M and Sadowski J 2001 *Acta Phys. Polon* A **100** 335
[24] Liu X, Sasaki Y and Furdyna J K 2001 *Appl. Phys. Lett.* **79** 2414
[25] Tanaka M and Higo Y 2001 *Phys. Rev. Lett.* **87** 026602
[26] Dietl T, Haury A and Merle d'Aubigné Y 1997 *Phys. Rev.* B **55** R3347
[27] Dietl T, Ohno H, Matsukura F, Cibert J and Ferrand D 2000 *Science* **287** 1019
[28] Dietl T, Ohno H and Matsukura F 2001 *Phys. Rev.* B **63** 195 205
[29] Lee B, Jungwirth T and MacDonald A H 2002 *Semicond. Sci. Technol.* **17** 393
[30] Ohno H 1999 *J. Magn. Magn. Mater.* **200** 110
[31] Twardowski A 2000 *Acta Phys. Polon* A **98** 203
[32] Matsukura F, Ohno H and Dietl T 2001 *Handbook of Magnetic Materials* ed K H J Buschow (Amsterdam: Elsevier) at press
[33] Cibert J, Ferrand D, H Boukari, Tatarenko S, Wasiela A, Kossacki P and Dietl T 2002 *Physica* E at press
[34] Kossacki P, Kudelski A, Gaj J A, Cibert J, Tatarenko S, Ferrand D, Wasiela A, Deveaud B and Dietl T 2002 *Physica* E at press
[35] Coey J M D, Viret M and von Molnár S 1999 *Adv. Phys.* **48** 167
[36] Tokura Y 2000 *Clossal Magnetoresistive Oxides* ed Y Tokura (London: Gordon and Breach)
[37] Dietl T, Śliwa C, Bauer G and Pascher H 1994 *Phys. Rev.* B **49** 2230
[38] Ohno H 1998 *Science* **281** 951
[39] Dietl T, Cibert J, Ferrand D and Merle d'Aubigné Y 1999 *Mater. Sci. Eng.* B **63** 103
[40] Balzarotti A, Motta N, Kisiel A, Zimnal-Starnawska M, Czyżyk M T and Podgórny M 1985 *Phys. Rev.* B **31** 7526
[41] Shioda R, Ando K, Hayashi T and Tanaka M 1998 *Phys. Rev.* B **58** 1100
[42] Langer J M, Delerue C, Lannoo M and Heinrich H 1988 *Phys. Rev.* B **38** 7723
[43] Blinowski J, Kacman P and Dietl T 2002 *Proc. Materials Research Society* at press webpage http://arXivorg/abs/cond-mat/0201012
[44] Zunger A 1986 *Solid State Phys.* vol 39 ed H Ehrenreich and Turnbull D (New York: Academic) p 275
[45] Zhang F C and Rice T M 1988 *Phys. Rev.* B **37** 3759
[46] Godlewski M, Świątek K and Suchocki A 1992 *J. Cryst. Growth.* **117** 634
[47] Benoit à la Guillaume C, Scalbert D and Dietl T 1992 *Phys. Rev.* B **46** 9853
[48] Mizokawa T and Fujimori A 1993 *Phys. Rev.* B **48** 14150
[49] Dietl T, Matsukura F and Ohno H 2001 webpage http://arXivorg/abs/cond-mat/0109245
[50] Głód P, Dietl T, Fromherz T, Bauer G and Miotkowski I 1994 *Phys. Rev.* B **49** 7797
[51] Furdyna J and Kossut J (eds) 1988 Diluted magnetic semiconductors *Semiconductors and Semimetals* vol 25 ed R K Willardson and A C Beer (New York: Academic)
[52] Kossut J and Dobrowolski W 1993 *Handbook of Magnetic Materials* vol 7 ed K H J Buschow (Amsterdam: Elsevier) p 231
[53] Dietl T 1994 *Handbook on Semiconductors* vol 3B ed T S Moss (Amsterdam: Elsevier) p 1251
[54] Schneider J, Kaufmann U, Wilkening W, Baeumler M and Köhl F 1987 *Phys. Rev. Lett.* **59** 240
[55] Masterov V F, Shtelmakh K F and Barbashov M N 1988 *Fiz. Tekh. Poluprovodn.* **22** 654 (Engl. Transl. 1988 *Sov. Phys. Semicond.* **22** 408)
[56] Szczytko J, Świątek K, Palczewska M, Twardowski A, Hayashi T, Tanaka M and Ando K 1999 *Phys. Rev.* B **60** 8304
[57] Bhattacharjee A K and Benoit à la Guillaume C 2000 *Solid State Commun.* **113** 17
[58] Szczytko J, Bardyszewski W and Twardowski A 2001 *Phys. Rev.* B **64** 075 306
[59] Okabayashi J, Kimura A, Rader O, Mizokawa T, Fujimori A, Hayashi T and Tanaka M 1998 *Phys. Rev.* B **58** R4211
[60] Okabayashi J, Kimura A, Rader O, Mizokawa T, Fujimori A, Hayshi T and Tanaka M 2001 *Phys. Rev.* B **64** 125 304
[61] Ohldag H, Solinus V, Hillebrecht F U, Goedkoop J B, Finazzi M, Matsukura F and Ohno H 2000 *Appl. Phys. Lett.* **76** 2928
[62] Ueda S, Imada S, Muto T, Saitoh Y, Suga S, Matsukura F and Ohno H 2001 *Physica* E **10** 210
[63] Masterov V F, Maltsev Yu V and Sobolevskii K K 1981 *Fiz. Tekh. Poluprovodn.* **15** 2127 (Engl. Transl. 1981 *Sov. Phys. Semicond.* **15** 1235)
[64] Sun H J, Peale R E and Watkins G D 1992 *Phys. Rev.* B **45** 8310, and references therein
[65] Kreissl J, Ulrici W, El-Metoui M, Vasson A-M, Vasson A and Gavaix A 1996 *Phys. Rev.* B **54** 10508
[66] Zając M, Dorandziński R, Gosk J, Szczytko J, Lefeld-Sosnowska M, Kamińska M, Twardowski A, Palczewska M, Grzanka E and Gębicki W 2001 *Appl. Phys. Lett.* **78** 1276
[67] Wołoś A, Palczewska M, Kamińska M and Twardowski A 2001 unpublished
[68] Blinowski J and Kacman P 2001 *Acta Phys. Polon.* A **100** 343
[69] Sato K and Katayama-Yoshida H 2001 *Jpn. J. Appl. Phys.* **40** L485
[70] Zener C 1951 *Phys. Rev.* **82** 403
[71] Park J H, Kwon S K and Min B I 2000 *Physica* B **169** 223

[72] Berciu M and Bhatt R N 2001 *Phys. Rev. Lett.* **87** 10723
See, however, Timm C, Schäffer F and von Oppen F 2001
webpage http://arXivorg/abs/cond-mat/0111504

[73] Sato K and Katayama-Yoshida H 2002 *Semicond. Sci. Technol.* **17** 367 and references therein

[74] Blinowski J, Kacman P and Majewski J A 1996 *Phys. Rev.* B **53** 9524

[75] J Blinowski, Kacman P and Majewski J A 1996 *J. Cryst. Growth* **159** 972

[76] Kępa H, Kutner-Pielaszek J, Twardowski A, Majkrzak C F, Sadowski J, Story T and Giebultwicz T M 2001 *Phys. Rev.* B **64** 121302(R)

[77] Belitz D and Kirkpatrick T R 1994 *Rev. Mod. Phys.* **57** 287

[78] Edwards P P and Rao C N R (eds) 1995 *Metal-Insulator Transitions Revisited* (London: Taylor and Francis)

[79] Pashitskii E A and Ryabchenko S M 1979 *Fiz. Tverd. Tela* **21** 545 (Engl. Transl. 1979 Sov. Phys. Solid State **21** 322)

[80] Wolff P A, Bhatt R N and Durst A C 1996 *J. Appl. Phys.* **79** 5196

[81] Bhatt R N and Wan X 1999 *Int. J. Mod. Phys.* C **10** 1459

[82] Inoue J, Nonoyama S and Itoh H 2000 *Phys. Rev. Lett.* **85** 4610

[83] Litvinov V I and Dugaev V K 2001 *Phys. Rev. Lett.* **86** 5593

[84] Gummich U and da Cunha Lima I C 1990 *Solid State Commun.* **76** 831

[85] Matsukura F, Ohno H, Shen A and Sugawara Y 1998 *Phys. Rev.* B **57** R2037

[86] Zener C 1951 *Phys. Rev.* **81** 440

[87] Zener C 1951 *Phys. Rev.* **83** 299

[88] Semenov Yu G and Ryabchenko S M 2001 *Physica* E **10** 165

[89] Fröhlich H and Nabarro F R N 1940 *Proc. R. Soc.* A **175** 382

[90] Edwards P P and Sienko M J 1978 *Phys. Rev.* B **17** 2575

[91] Oiwa A, Katsumoto S, Endo A, Hirasawa M, Iye Y, Ohno H, Matsukura F, Shen A and Sugawara Y 1997 *Solid State Commun.* **103** 209

[92] Katsumoto S, Oiwa A, Iye Y, Ohno H, Matsukura F, Shen A and Sugawara Y 1998 *Phys. Status Solidi* B **205** 115

[93] Shirai M 1999 unpublished

[94] Paalanen M A and Bhatt R N 1991 *Physica* B **169** 223

[95] Głód P, Dietl T, Sawicki M and Miotkowski I 1994 *Physica* B **194-196** 995

[96] Nagai Y, Kunimoto T, Nagasaka K, Nojiri H, Motokawa M, Matsukura F, Dietl T and Ohno H 2001 *Jpn. J. Appl. Phys.* **40** 6231

[97] Katsumoto S *et al* 2001 *Mater. Sci. Eng.* B **84** 88

[98] Potashnik S J, Ku K C, Chun S H, Berry J J, Samarth N and Schiffer P 2001 *Appl. Phys. Lett.* **79** 1495

[99] Kenett M P, Berciu M and Bhatt R N 2001 webpage http://arXivorg/abs/cond-mat/0102315

[100] Leroux-Hugon P 1973 *New Developments in Semiconductors* ed P R Wallace, R Harris and M J Zuckermann (Leyden: Noordhoff) p 63

[101] Jungwirth T, Atkinson W A, Lee B H and MacDonald A H 1999 *Phys. Rev.* B **59** 9818

[102] Lee B, Jungwirth T and MacDoland A H 2000 *Phys. Rev.* B **61** 15 606

[103] Abolfath M, Jungwirth T, Brum J and MacDonald A H 2001 *Phys. Rev.* B **63** 054 418

[104] Dietl T, König J and MacDonald A H 2001 *Phys. Rev.* B **64** R241 201

[105] König J, Lin H-H and MacDonald A H 2000 *Phys. Rev. Lett.* **84** 5628

[106] König J, Jungwirth T and MacDonald A H 2001 *Phys. Rev.* B **64** 184423

[107] König J, Schliemann J, Jungwirth T and MacDonald A H 2001 webpage http://arXivorg/abs/cond-mat/0111314

[108] Zarand G and Janko B 2001 webpage http://arXivorg/abs/cond-mat/0108477

[109] Eggenkamp P T J, Swagten H J M, Story T, Litvinov V I, Swuste C H W and de Jonge W J M 1995 *Phys. Rev.* B **51** 15 250

[110] Fisher M E, Ma S-k and Nickel B G 1972 *Phys. Rev. Lett.* **29** 917

[111] Schliemann J, König J, Lin H-H and MacDonald A H 2001 *Appl. Phys. Lett.* **78** 1550

[112] Chattopadhyay A, Das Sarma S and Millis A J 2001 *Phys. Rev. Lett.* **87** 227 202

[113] Schliemann J, König J and MacDonald A H 2001 *Phys. Rev.* B **64** 165 201

[114] Chudnovskij A L and Pfannkuche D 2001 webpage http://arXivorg/abs/cond-mat/0108396

[115] Bhatt R N, Berciu M, Kennett M P and Wan X 2001 webpage http://arXivorg/abs/cond-mat/0111184

[116] Ando K, Hayashi T, Tanaka M and Twardowski A 1998 *J. Appl. Phys.* **83** 6548

[117] Szczytko J, Mac W, Twardowski A, Matsukura F and Ohno H 1999 *Phys. Rev.* B **59** 12935

[118] Beschoten B, Crowell P A, Malajovich I, Awschalom D D, Matskura F, Shen A and Ohno H 1999 *Phys. Rev. Lett.* **83** 3073

[119] Omiya T, Matsukura F, Dietl T, Ohno Y, Sakon T, Motokawa M and Ohno H 2000 *Physica* E **7** 976

[120] Andrearczyk T *et al* 2001 *Proc. 25th Int. Conf. on Physics of Semiconductors (Osaka, Japan, 2000)* ed N Miura and T Ando (Berlin: Springer) p 235

[121] Sawicki M, Hansen L, Ferrand D, Molenkamp L W, Waag A, Le Van Khoi and Dietl T 2002 *Phys. Status Solidi* B **229** 717

[122] Oiwa A, Słupiński T and Munekata H 2001 *Appl. Phys. Lett.* **78** 518

[123] von Molnár S, Munekata H, Ohno H and Chang L L 1991 *J. Magn. Magn. Mater.* **93** 356

[124] Satoh Y, Okazawa D, Nagashima A and Yoshino J 2001 *Physics* E **10** 196

[125] Overberg M E, Abernathy C R, Pearton S J, Theodoropoulou N A, MacCarthy K T and Hebard A F 2001 *Appl. Phys. Lett.* **79** 1312

[126] Munekata H, Zaslavsky A, Fumagalli P and Gambino R J 1993 *Appl. Phys. Lett.* **63** 2929

[127] Ohno H, Matsukura F, Shen A, Sugawara Y, Oiwa A, Endo A, Katsumoto S and Iye Y 1996 *Proc 23rd Int. Conf. on the Physics of Semiconductors (Berlin 1996)* ed M Scheffler and R Zimmermann (Singapore: World Scientific) p 405

[128] Shen A, Ohno H, Matsukura F, Sugawara Y, Akiba N, Kuroiwa T, Oiwa A, Endo A, Katsumoto S and Iye Y 1997 *J. Cryst. Growth* **175-176** 1069

[129] Fedorych O M, Hankiewicz E M, Wilamowski Z and Sadowski J 2001 webpage http://arXivorg/abs/cond-mat/0106227

[130] Shono T, Hasegawa T, Fukumura T, Matsukura F and Ohno H 2000 *Appl. Phys. Lett.* **77** 1363

[131] Hubert A and Schafer R 1998 *Magnetic Domains* (Berlin: Springer)

[132] Park Y D, Hanbicki A T, Erwin S C, Hellberg C S, Sullivan J M, Mattson J E, Ambrose T F, Wilson A, Spanos G and Jonker B T 2002 *Science* **295** 651

[133] Overberg M E, Gila B P, Abernathy C R, Pearton S J, Theodoropoulou N A, MacCarthy K T, Arnason S B and Hebard A F 2001 *Appl. Phys. Lett.* **79** 3128

[134] Kuwabara S, Kondo T, Chikyow T, Ahmet P and Munekata H 2001 *Jpn. J. Appl. Phys.* **40** L724

[135] Theodoropolpu N, Hebard A F, Overberg M E, Abernathy C R, Pearton S J, Chu S N G and Wilson R G 2001 *Appl. Phys. Lett.* **78** 3475

[136] Sonoda S, Shimizu S, Sasaki T, Yamamoto Y and Hori H 2001 webpage http://arXivorg/abs/cond-mat/0108159

[137] Reed M L, El-Masry N A, Stadelmaier H H, Ritums M K, Reed M J, Parker C A, Roberts J C and Bedair S M 2001 *Appl. Phys. Lett.* **79** 3473

[138] Pekarek T M, Crooker B C, Miotkowski I and Ramdas A K 1998 *J. Appl. Phys.* **83** 6557

[139] Medvedkin G A, Ishibashi T, Nishi T, Hayata K, Hasegawa Y and Sato K 2000 *Jpn. J. Appl. Phys.* **39** L949

[140] Kamatani T and Akai H 2001 *Physica* E **10** 157

[141] Kacman P 2001 *Semicond. Sci. Technol.* **16** R25

[142] Ueda K, Tabata H and Kawai T 2001 *Phys. Lett.* **79** 988

[143] Saeki H, Tabata H and Kawai T 2001 *Solid State Commun.* **120** 439

[144] Matsumoto Y, Murakami M, Shono T, Hasegawa T, Fukumura T, Kawasaki M, Ahmet P, Chikyow T, Koshihara S and Koinuma H 2001 *Science* **291** 854

[145] Dietl T 1994 *Handbook on Semiconductors* vol 3B ed T S Moss (Amsterdam: North-Holland) p 1327

[146] Yokota T, Fujimura N, Morinaga Y and Ito T 2001 *Physica* E **10** 237

[147] Hellman F, Queen D R, Potok R M and Zink B L 2000 *Phys. Rev. Lett.* **84** 5411

[148] Isber S, Fau C, Chaar S, Averous M and Golacki Z 1995 *Mater. Sci. Forum* **182-184** 657

[149] Young D P, Hall D, Torelli M E, Fisk Z, Sarrao J L, Thompson J D, Ott H-R, Oseroff S B, Goodrich R G and Zysler R 1999 *Nature* **397** 412

[150] Makarova T L, Sundqvist B, Höhne R, Esquinazi P, Kapelevich Y, Scharff P, Davydov V A, Kashevarova L S and Rakhmanina A V 2001 *Nature* **413** 716

[151] Vurgaftman I, Meyer J R and Ram-Mohan L R 2001 *J. Appl. Phys.* **89** 5815